Chapter 2
Nanosensors for Intracellular Raman Studies

Patrick I.T. Thomson and Colin J. Campbell

Abstract Raman spectroscopy is an increasingly exploited tool for the study of cell biology, and the focus of this chapter is surface-enhanced Raman spectroscopy (SERS). Using SERS, noble metal nanoparticles can be interrogated with wavelengths of light to which cells exhibit minimal autofluorescence and return useful information about their immediate chemical environment. Using established gold–thiol surface chemistry, gold nanoparticles can be functionalised with suitable reporter molecules used to make nanosensors, which can be chosen to be sensitive to intracellular variables such as pH, protein concentration/activity or redox potential. This chapter presents the general concept of SERS for use in the monitoring of intracellular variables, and we will describe the preparation, use and functions of the nanosensors.

2.1 Background: Intracellular Nanosensors

The chemical environment inside cells is of great interest, and many methods are known which can destructively assay properties such as redox potential [1] or the concentration of arbitrary metabolites [2]. However, if such information is desired about the progress of individual cells over time, or living tissues, then non-destructive methods of obtaining information are needed. Fluorescent sensors are widely used [3, 4], with fluorescent proteins and fluorescent nanoparticles being particularly popular because they can be engineered to respond to an environmental stimulus and report it as a measurable change in fluorescence (which is a well-established modality in cellular imaging). Nanoparticles are well suited since they are readily taken up by cells, and techniques to engineer the architecture and

P.I.T. Thomson • C.J. Campbell (✉)
EaStCHEM School of Chemistry, University of Edinburgh, Edinburgh EH9 3JJ, UK
e-mail: patrick.thomson@gmail.com; colin.campbell@ed.ac.uk

S. Li et al. (eds.), *Nanoscale Sensors*, Lecture Notes in Nanoscale Science and Technology 19, DOI 10.1007/978-3-319-02772-2_2,

composition of nanoparticles are well established. Fluorescent proteins exhibit a complementary set of benefits; cells can be engineered to stably express them and genetic engineering techniques can be used to modify their function. However, fluorescence-based methods have limitations, such as background fluorescence of the cell and medium limiting the lower limits of detection, and the requirement of a photoactivatable electronic transition which is sensitive to environmental conditions. Raman spectroscopy and imaging offers an alternative to fluorescence, and in this chapter, we provide some examples where the features of Raman spectroscopy can be used to the benefit of the experimentalist.

2.2 Background: Raman and SERS

When photons are scattered by an atom or molecule, most of the light is reemitted unchanged (elastic or Rayleigh scattering). These resultant photons have the same kinetic energy as the incident ones, and are responsible for such phenomena as the colour of the sky [5]. However, approximately one in ten million reemitted photons have a different (usually lower) kinetic energy to the one absorbed (inelastic or Stokes Raman scattering)—indicating that the target molecule has undergone a transition in vibrational energy levels (Fig. 2.1) [6]. The frequency shift in these photons can be directly correlated to vibrational energy levels and thus gives us information about the vibrational modes of the target molecule in a similar fashion to infrared spectroscopy. The phenomenon was first observed and described by Sir Venkata Rāman, for which he was knighted and subsequently awarded the Nobel Prize in Physics in 1930 [7].

Raman and infrared spectroscopy can both probe the vibrational modes of target molecules, but the two techniques have the potential to return complementary information due the differing selection rules that govern which vibrational modes are IR

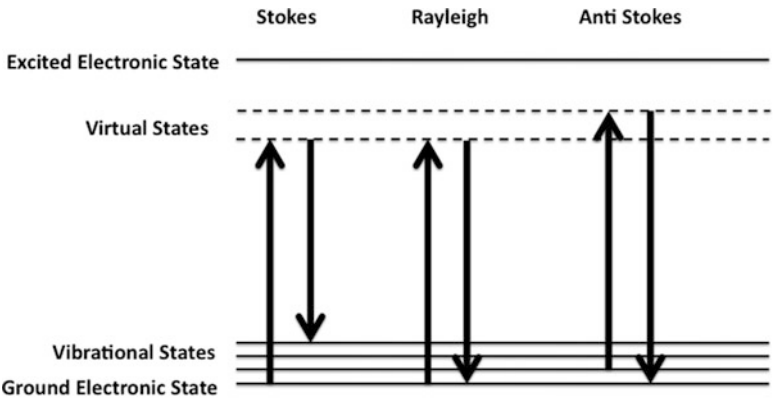

Fig. 2.1 Scattering modes for the interaction of photons with matter

active and which are Raman active. The main drawback of Raman spectroscopy is its low sensitivity—and the complex techniques thus required to separate out the Raman-scattered photons from the much more intense Rayleigh background [6].

The utility of Raman spectroscopy received a boost in 1974, when a phenomenon called surface-enhanced Raman spectroscopy (SERS) was first observed by Fleischmann [8, 9]. Specifically, he observed an anomalous enhancement of the Raman spectrum of pyridine adsorbed onto the surface of a roughened silver electrode. Theories to explain the phenomenon were proposed concurrently by Van Duyne [10] and Creighton [11], with the predominant theory today being Van Duyne's proposed involvement of surface plasmon resonance. Incident light on a metallic surface can excite localised surface plasmons, which increases the local electric field and can enhance the Raman scattering of adsorbed molecules by a factor ranging from 4 to 14 orders of magnitude [12–15]. Silver and gold surfaces and nanoparticles are particularly useful substrates for SERS studies of biological systems since they are relatively inert and the wavelength required to excite their surface plasmons falls in the visible/near-IR range, to which biological systems are permeable [16]. For spherical homogeneous nanoparticles, the SERS signal is greatest when they are clustered together; the nanoparticle–nanoparticle junction experiences a localised enhancement in plasmon intensity, and this dominates signals from single nanoparticles. Various strategies have been developed in order to use single nanoparticles as effective SERS sensors without relying on aggregation, such as dielectric-cored gold nanoshells [17], gold nanorods or gold nanostars [18]. Exploiting these features, the SERS enhancement in some cases can permit the detection of single molecules [13, 19].

2.3 SERS Measurements in Cells

As a result of the high sensitivity, SERS is a very useful technique for measuring the Raman spectra of small numbers of molecules [19] or nanoparticles, and as a result it has been used to explore the environment inside individual cells. Even a single gold nanoparticle can return useful spectral information about analytes close to its surface, and this has been used to probe the internal environments of both bacterial [20] and eukaryotic [21, 22] cells directly. To use SERS in this way, it is necessary to know where in the cell the nanoparticle locates and whether its presence has any detrimental effect on the cell (e.g., does it cause stress or induce cell death?).

Gold nanoparticles delivered to cells in this manner do not typically affect cell viability, and we have demonstrated that they do not induce cell death (either apoptotic or necrotic) or cause oxidative stress. Cellular uptake of gold nanoshells [22] is dependent on a variety of factors. We tested various culture conditions in order to probe different endocytosis mechanisms (e.g., by depleting clathrin, cholesterol or ATP from the cells), but we found that the greatest level of cellular delivery is when using cell culture media containing no calf serum (Fig. 2.2). We attribute this finding to the fact that serum proteins are known to coat nanoparticles,

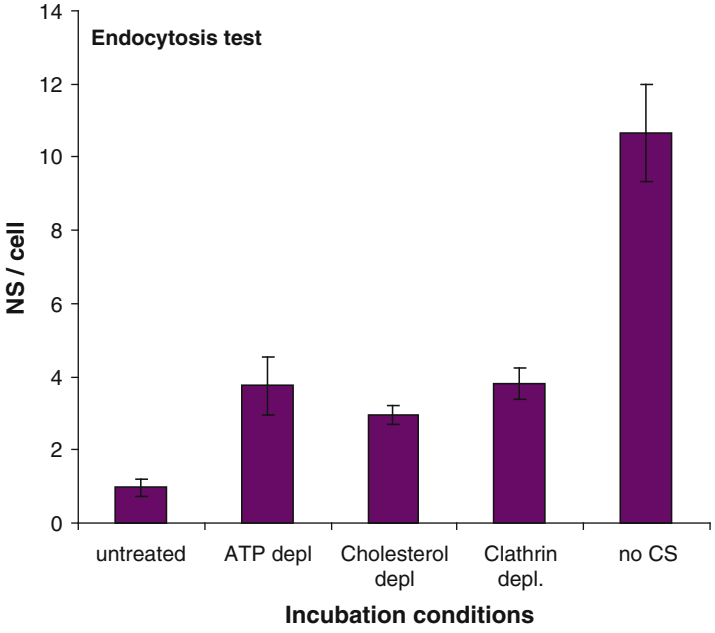

Fig. 2.2 Estimated amount of NS per cell according to particles found in 100 TEM sections. NS incubations for this test were conducted for 5 h with 10 fm NS in 10 % calf serum (CS)-containing media, except the condition with no CS on the far *right*. The *bars* show the amount of NS (monomers, dimers) found in 100 cell sections

thus changing their physicochemical surface characteristics. This change in surface characteristics seems to be sufficient to change the way in which some cell types react to the nanoshells.

An important consequence of removing serum proteins from the culture medium is that the nanoshells which are taken up tend to be more likely to be free in the cytosol, whereas those taken up in the presence of serum are more likely to be found in endosomal structures. Figure 2.3 shows TEM images of gold nanoshells in different locations within mouse fibroblast cells. In Fig. 2.3a, b, nanoshell dimers are encapsulated in endosomes as a result of incubation in serum-containing culture media. Similarly Fig. 2.3c shows a nanoshell which had been incubated in serum-containing media coated in a biomolecular corona. Only in serum-free conditions (Fig. 2.3d) can the nanoshells be seen free in the cytosol.

When we used gold nanoshells [17] to measure SERS spectra inside cells, we found that the spectra contained peaks characteristic of a variety of biomolecular vibrational modes, mostly originating from proteins. Examples of these spectra can be seen in Fig. 2.4. Specifically, Fig. 2.4 shows two important features. Firstly, while spectra b–e show the heterogeneity between SERS spectra measured at different spatial locations within the cell, they do not show any vibrations characteristic of nucleic acids—this suggests that the nanoshells do not access the nucleus. Secondly,

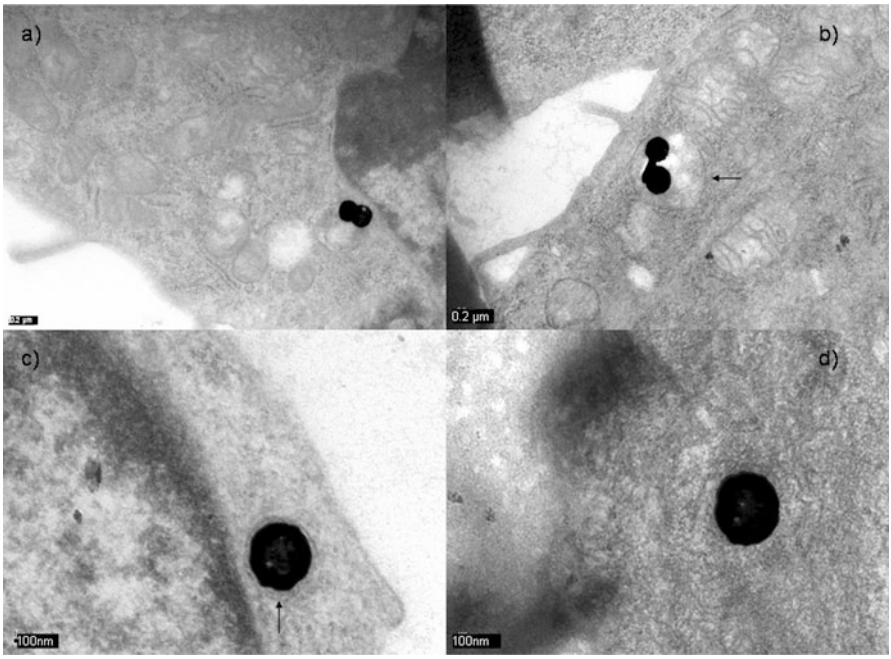

Fig. 2.3 Set of TEM images of NS inside cells. Images (**a**, **b**, **c**) are all of NS which were incubated in media containing 10 % CS and can be found either (**a**) free suspended in the cytosol (scalebar 0.2 µm) or (**b**) taken up in oversized vesicles or as in (**c**) surrounded by what may be a dense coating of protein. (**d**) Representative NS which has been taken up during incubation without any CS in the growth media. None of the NS found in these conditions were surrounded by any kind of coating or vesicles inside the cells

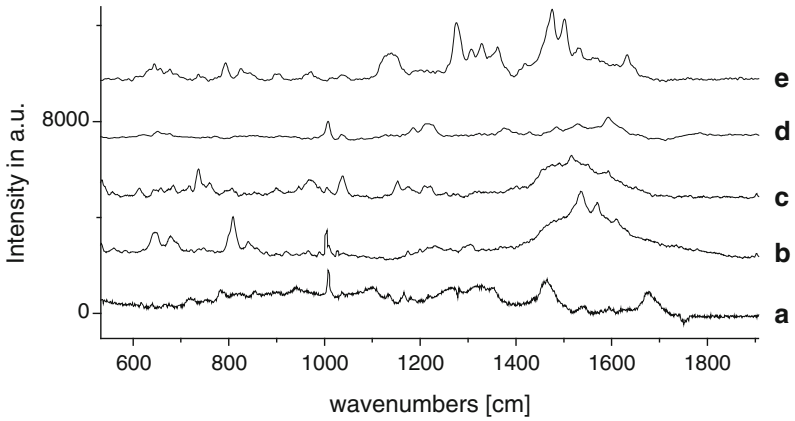

Fig. 2.4 (**a**) Averaged Raman spectrum of 50 different NIH/3T3 fibroblast cells measured at a 785.32 nm excitation wavelength, 50 mW laser power at the sample for 180 s. (**b**–**e**) SER spectra taken by excitation of NS in different cells at the same wavelength with 5 s acquisition time and 3 mW laser power at the sample

Table 2.1 Vibrational modes and assignments in the Raman spectra of cellular contents as shown in Fig. 2.4. SERS-enhanced signals from samples b–e are correlated with the assigned peaks in the whole-cell Raman spectrum

		NS in different cells (cm^{-1})			
Whole-cell resonance (cm^{-1})	Assignment of Raman features	(b)	(c)	(d)	(e)
640	C–C twist in tyrosine	646		642	644
675	C–S stretch in cysteine	678	684		
720	C–N stretch in lipid/adenine		736		737
783	DNA: O–P–O backbone stretch in thymine/cytosine				
825	DNA: O–P–O backbone stretch/out of plane ring breath in tyrosine				825
856	In plane ring breathing mode in tyrosine/C–C	848		850	
893	C–C skeletal stretch in protein		900	905	896
941	C–C skeletal stretch in protein		967		972
1,008	Symmetric ring breathing mode of phenylalanine	1,005	1,005	1,007	1,428
1,036	C–H in plane bending mode of phenylalanine		1,037	1,038	1,036
1,100	DNA: O–P–O backbone stretching				
1,109	DNA: O–P–O backbone stretching				
	C–N stretch in polypeptide chains		1,133	1,138	1,139
1,166	C–C stretching in proteins	1,174	1,174		
1,217	Amide III: beta-sheet	1,216	1,209	1,214	1,214
1,266	Amide III: beta-sheet/adenine/cytosine				1,275
1,329	Guanine			1,323	1,329
1,354	Polynucleotide chain (DNA bases)				
	Possible porphyrin stretches			1,375	1,366
1,465	(ν (C = C) + ν(C − C) + ν(C = O − H)), Chromophore			1,485	1,475
	Aromatic ring stretches		1,516		1,511
1,543	Lipid stretches	1,535		1,528	1,534
	Tyrosine stretch	1,570		1,593	1,570
1,595	Ring mode (adenine/guanine)				
1,619	C═C bending in phenylalanine and tyrosine	1,616			
1,677	Amide I: alpha-helix				

a comparison of the bulk Raman signal from cells (Fig. 2.4a) with SERS spectra (Fig. 2.4b–e) shows the intensity of the SERS effect. The bulk Raman measurement is only possible by using high laser powers, long acquisition times and averaging over several cells; SERS measurements are made using low laser power and short acquisition times and have subcellular resolution. Table 2.1 shows the peak positions and assignments of vibrational modes typically recorded when measuring Raman spectra in cells.

2.4 SERS Nanosensors

For constructing SERS nanosensors, gold and silver are the most popular nanoparticle substrates by far [18]. The use of these metals, particularly gold, means that surface functionalisation of the nanoparticles can be relatively simple. Sulphur and gold exhibit a specific interaction in which organic thiols and disulfides spontaneously ligate onto a gold surface and form a monolayer, under ambient conditions from dilute aqueous or organic solutions [23–25]. In this way, monolayer surfaces of organic molecules can be constructed to put them in contact with both a gold nanoparticle surface and the surrounding environment, so that each probe molecule is presented with the same chemical environment. Thus, all the necessary requirements for a nanosensor are fulfilled: the molecules are SERS active, they are stably attached to the particles, and the sensors report on their environment. Delivering the assembled nanosensors into a cell is usually extremely simple; incubating eukaryotic cells with a high-femtomolar concentration of nanosensors in serum-free media is usually sufficient to cause uptake directly and without affecting cell viability [22]. Additionally, nanosensor distribution in cells is found to be directly proportional to the extracellular concentration, giving an easy way to tune intracellular sensor density. This is in sharp contrast to methods using modified fluorescent proteins, which require the genetic engineering of specific cell lines.

In general, a sensor is a system which detects a particular stimulus by changing its properties in a measurable manner; SERS sensors typically consist of a metal nanoparticle substrate, functionalised with a reporter molecule adsorbed on the surface. The functionalised nanoparticle can act as both a delivery mechanism and as a SERS-active surface for monitoring, and the reporter molecule typically has a structure sensitive to a particular stimulus. When the structure of the reporter molecule changes, so does its Raman spectrum, and so comparison of different regions of the Raman spectrum will give a direct read-out of the relative proportions of a reporter in its distinct conformational states—and this can be calibrated with, e.g., buffers with known analyte concentration or of known pH or redox potential (Fig. 2.5).

This type of sensor is distinct from the majority of fluorescent reporters which exhibit an irreversible change in fluorescence as a result of a covalent reaction with an analyte. For example, DCFH-DA is a fluorescent dye commonly used for the detection of reactive oxygen species (ROS). In the presence of ROS, it switches from a nonfluorescent dihydrodichlorofluorescein to the fluorescent form, dichlorofluorescein. While this gives important information on the formation of ROS, the reaction is irreversible and as a result the reporter cannot report on a change back to low ROS concentrations. Similarly, “sandwich assays” which use two probe molecules in order to measure analyte concentrations (one of which is labelled with a fluorescent reporter) are irreversible and cannot measure dynamic changes in concentration of an analyte.

Sandwich assays are typically used to measure concentrations of molecules such as proteins, and we recently developed a SERS nanosensor for the detection of

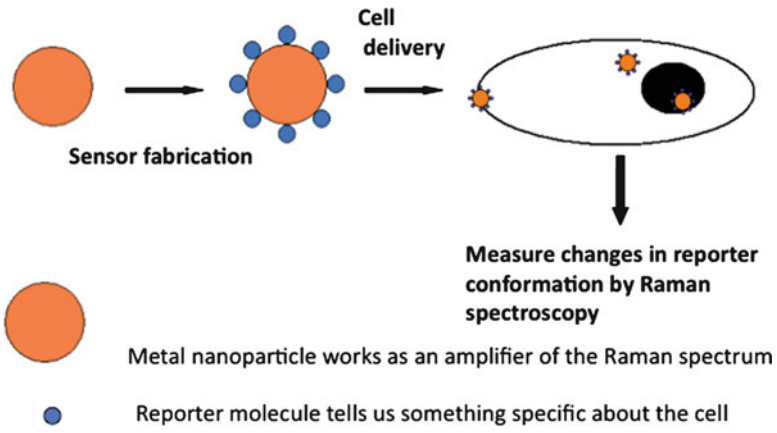

Fig. 2.5 Schematic for intracellular SERS sensing

the protein thrombin. Thrombin is an important target molecule clinically since it is an important regulator of the cascade of reactions which lead to blood clot formation. Blood clots cause an estimated 25,000 deaths in the UK per year and recent clinical guidelines have suggested that evaluation of the risk of clot formation could significantly reduce this toll [26, 27]. A simple, sensitive test of thrombin levels could be a valuable tool in such evaluations.

2.5 Nanosensors: Protein Quantification

In a recent paper, we considered that an aptamer, specific for thrombin (referred to herein as TBA), would be a probe molecule well suited to SERS sensors [28]. Aptamers are probe molecules made from nucleic acid oligomers, which have been selected (via a process called SELEX) for their ability to bind non-nucleic acid target molecules. Since aptamers often undergo a conformational change on binding their cognate target and since the probe and target are physicochemically distinct (nucleic acid and protein respectively), we predicted that we would see a change in the SERS spectrum as a result of thrombin binding to TBA immobilised on the surface of a gold nanoshell (shown schematically in Fig. 2.6).

The thrombin nanosensor was assembled from gold nanoshells which were surface functionalised with TBA, then the remaining surface blocked with mercaptohexanol (MCH). MCH blocking allows better sensitivity in the sensor since it inhibits non-specific binding to the gold surface and therefore inhibits non-specific signals such as those seen in Fig. 2.4. The Raman spectra from the nanosensors show very low intensity (Fig. 2.7), with a prominent and stable feature at 1,089 cm^{-1} assignable to the DNA O–P–O backbone stretch, and this does not change when the nanosensor is incubated with either bovine serum albumin (BSA),

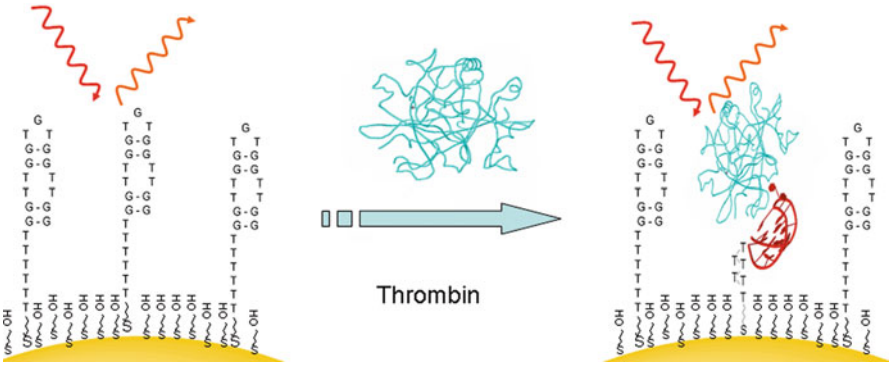

Fig. 2.6 The assembled mixed monolayer of prehybridised TBA oligonucleotide and MCH and the model for the detection

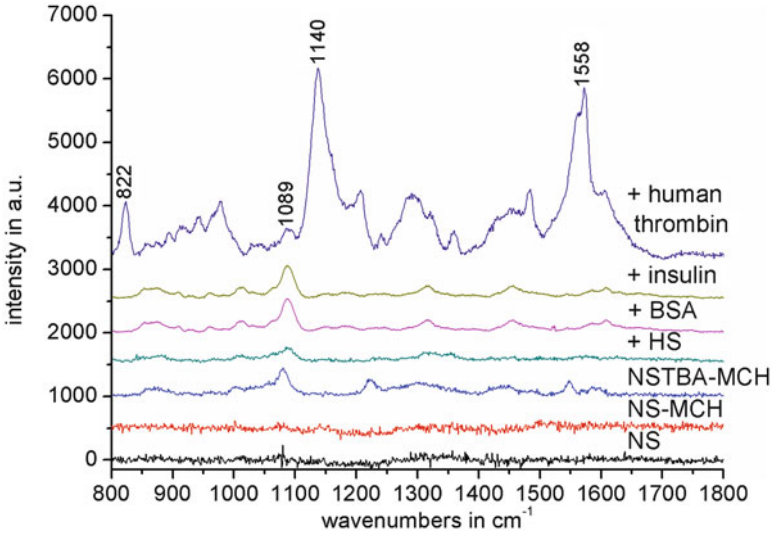

Fig. 2.7 SERS spectra from thrombin nanosensor. The *top trace* shows the spectrum measured as the result of a specific interaction between thrombin and TBA—dominant peaks can be assigned to DNA vibrational modes (see text). Controls with BSA (10 mg/ml), insulin 600 nM and 1 % human serum show no evidence of protein binding. Lower three spectra show spectra of NS, NS plus blocking agent (mercaptohexanol) and the fully assembled NSTBA sensor. Spectra are averages of ten acquisitions

human serum (HS) or insulin—this shows that there is very little signal change associated with non-specific binding of non-cognate proteins to the nanosensor. On incubation with its cognate target (thrombin), there is a large change in the nanosensor SERS spectrum. The major spectral changes include increases in signal at 822, 1,140 and 1,558 cm^{-1}. These can be assigned to the combined C2′-endo and C3′-endo modes of the 2′-deoxyribose sugars, the C–O–C stretch at 1,140 cm^{-1}

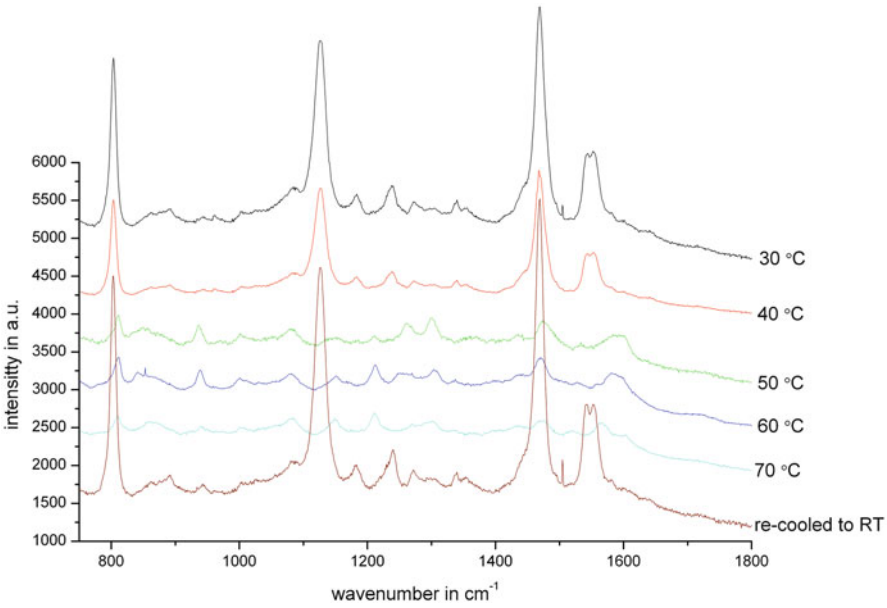

Fig. 2.8 SERS spectra of a G-quadruplex forming oligonucleotide. Heating and cooling cycles show that the secondary structure can be reversibly disrupted allowing a structural switch

and guanine ring modes at 1,558 cm^{-1}. At 1,480 cm^{-1} the low intensity feature can be assigned to a guanine ring mode [29, 30]. Further signal increases can be assigned to vibrational modes of protein, such as the amide III backbone vibration at 1,220 cm^{-1}, CH_2 stretching mode at 1,440–1,460 cm^{-1} or tyrosine aromatic ring vibrations at 1,610 cm^{-1} [31, 32]. When we used an oligonucleotide with no specific affinity for thrombin, we saw no change in its SERS signal—this confirms that the spectral change correlates with a specific interaction between TBA and thrombin.

Our investigations showed that the majority of the spectral change could be attributed to the formation of a G-quadruplex motif in the aptamer structure, and to prove this, we functionalised NS with an oligonucleotide known to form a G-quadruplex structure. Not only was its spectrum very similar to that of the TBA–thrombin complex, but controlled heating demonstrated that the secondary structure was responsible for the strong spectral signals and that the structure reformed on cooling (Fig. 2.8). We also showed that the sensor response to thrombin scaled with concentration and that we could detect low, clinically relevant concentrations (Fig. 2.9).

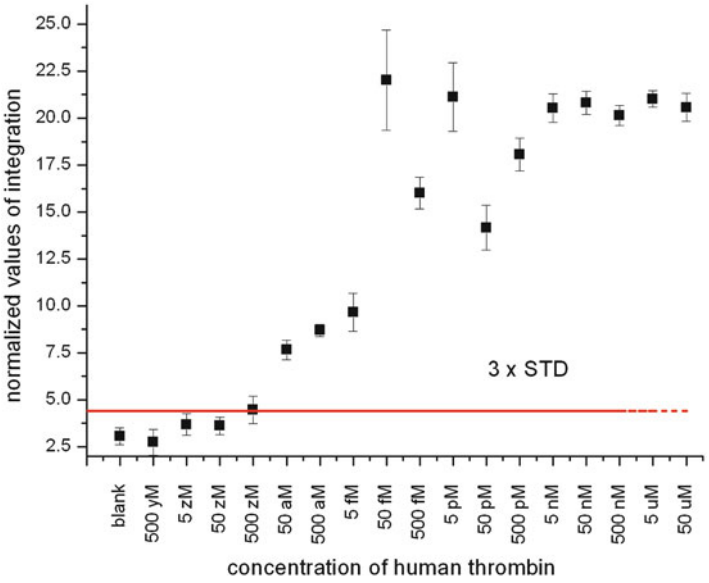

Fig. 2.9 Calibration curve for thrombin detection. *Error bars* represent single standard deviations

2.6 Nanosensors: Peptide Structure and Protease Activity

In a subsequent publication we adapted the concept of using SERS to investigate biomolecular structure in order to study the potential dependence of the structure of a peptide implicated in Goodpasture's disease and furthermore to determine how the peptide structure altered its interaction with a protease (cathepsin D) [33]. Goodpasture's disease is a rare autoimmune condition of the kidneys and lungs in which there is an immune response to a misfolded domain of the alpha-3 chain of type IV collagen (α3(IV)NC1$_{67–85}$). It is thought that in healthy individuals α3(IV)NC1$_{67–85}$ is completely broken down (destructive processing) [34] and as a result is never normally presented to T cells. Destructive processing of the antigen is thought to require reduction of a disulfide bridge that holds it in a hairpin-like conformation, which is then followed by proteolytic cleavage by an aspartate protease, cathepsin D [35, 36]. The importance of the oxidation state of the cysteine thiols in the peptide suggests that the redox environment during α3(IV)NC1$_{67–85}$ processing may be crucial in determining whether processing proceeds as described with destruction of α3(IV)NC1$_{67–85}$ or some other route in which α3(IV)NC1$_{67–85}$ is preserved and autoreactive T cells are activated. It is therefore important to determine the standard redox potential of the disulfide bond of the peptide and investigate how redox potential influences proteolysis.

Since we had shown the utility of SERS in determining the conformation of an oligonucleotide, we speculated that SERS could similarly be used to determine

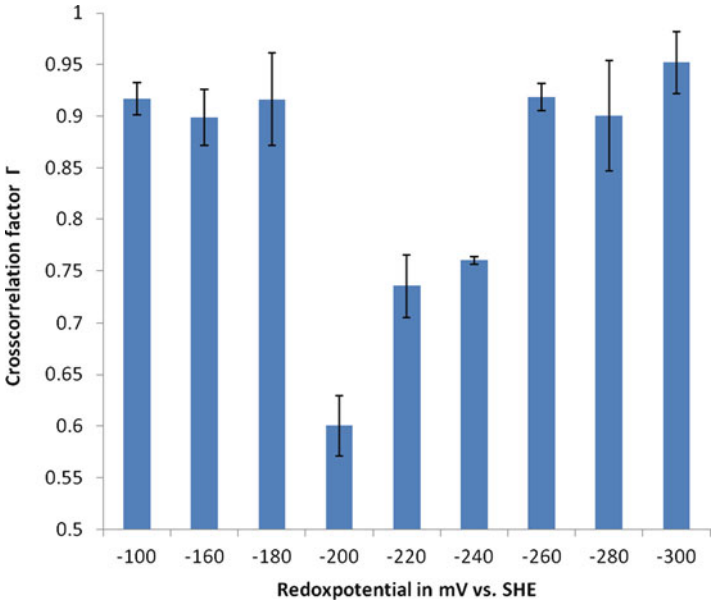

Fig. 2.10 Graph showing diagonal cross-correlation factors Γ (correlating 25 spectra) versus redox potential from −100 to −300 mV. Values close to 1 describe conformational stability and decreasing Γ values depict a dynamic conformational change. The dip at −200 mV suggests the dynamic breaking and formation of the internal disulfide bond of AS35. The *error bars* describe a single standard deviation over three independent experiments

the conformation (and therefore the oxidation state) of a peptide. In order to measure SERS spectra from the peptide, we made a nanosensor from the peptide (attached via a free cysteine at its c-terminus) to gold nanoshells. We controlled the solution redox potential (E) using defined pH and concentrations of glutathione and glutathione disulfide in accordance with the Nernst equation for glutathione (where E^{θ} is the standard redox potential for glutathione/glutathione disulfide):

$$E = E^{\theta} + \frac{RT}{nF} \ln \frac{[GSSG]\,[H^{+}]^{2}}{[GSH]^{2}}$$

and measured the cross-correlation factor between consecutive spectra (Γ), which we suggest is a reporter of population heterogeneity

At reducing potentials the peptide molecules should be a homogeneous population in a hairpin structure, at oxidising potentials the peptide molecules should be a homogeneous population in a linear structure and at intermediate potentials the molecules should be a heterogeneous mixture. This is indeed what we see (Fig. 2.10) with a pronounced dip in Γ at around −200 mV versus NHE.

This conformational change also correlated well with the digestion of the peptide by the protease cathepsin D. By controlling redox potential and measuring

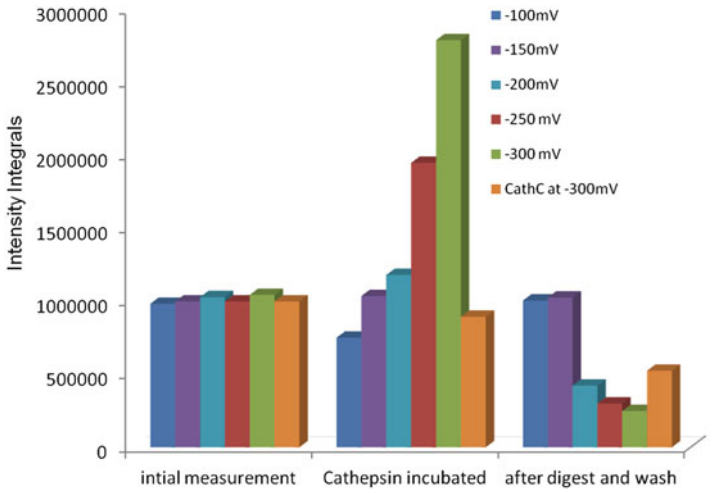

Fig. 2.11 Integrals from spectra recorded during digestion experiments at redox potentials of −100, −250 and −300 mV and control experiments with less active protease cathepsin C and pepstatin A inhibited cathepsin D at −300 mV, compared before, during and after the incubation with cathepsin

SERS before, during and after addition of the protease, we could measure both binding of the protease during digestion and the loss of specific peptide signal as a result of digestion (Fig. 2.11). Significantly, the addition of pepstatin A (an inhibitor of cathepsin D) stopped any digestion of the peptide. Taken together these findings suggest that dysregulation of redox potential can lead to defective antigen processing. When the antigen is improperly processed, this can lead to the autoimmune reaction that causes degeneration of kidney and lung tissue.

2.7 pH-Sensitive Intracellular SERS Nanosensors

When the functionalised nanoparticles are delivered inside cells, they act as nanosensors and can measure physiologically interesting events in single live cells in real time (Fig. 2.5). The first and most well-explored class of intracellular SERS nanosensors have been those sensitive to changes in pH. For the measurement of pH, reporter molecules should incorporate an acid or basic group which is sensitive to pH changes and a thiol group for ligation to a metal nanoparticle. The protonation state of the probe molecule can then be used to calculate the pH via the Henderson–Hasselbalch equation. The range of this type of sensor is determined by the pK_a of the reporter molecule attached to the particle, and so careful selection of the probe molecule can give sensors sensitive to different ranges of pH and therefore be useful in different applications (Fig. 2.12).

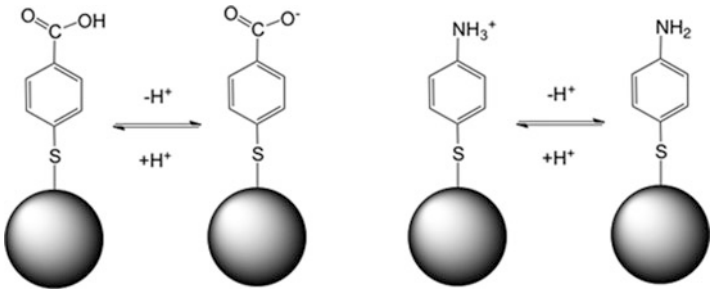

Fig. 2.12 Two different types of pH-responsive nanosensors sensitive to base (*left*) and acid (*right*)

The first pH-sensitive SERS nanosensor was designed for the measurement of pH in living cells using silver nanoparticles [37]. The sensor used 4-mercaptobenzoic acid as reporter, which ligated to the metal surface via the thiol group, and was responsive to pH ranging from 6 to 8 pH units due to the carboxylic acid. However, the SERS enhancement was found to originate solely from clusters of nanoparticles, which also exhibit a large variability in the electrical double layer close to the nanoparticle–nanoparticle junctions and thus the local pH. Unfortunately these nanoparticle–nanoparticle junctions are also SERS "hotspots" and the measurements, though accurate, encompass individual reporter molecules over widely varying local pH values. For these reasons, the nanosensor suffered from a wide variability in the reported pH (± 1 pH unit). Use of gold nanoshells [22, 38] overcame the problem with aggregation, as these engineered particles comprising a dielectric silica core coated in a film of gold gave a further enhancement of the Raman signal from the surface monolayer of 4-mercaptobenzoic acid. In this way, single nanoparticles still act as effective nanosensors and the "hotspots" created by nanoparticle–nanoparticle junctions no longer overwhelm the signal from the rest of the surface reporter molecules. The pH resolution could be improved to ± 0.1 pH units over the range of 5.8–7.6 pH units, but with some sensitivity between 4 and 9 pH units.

As well as carboxylic acid probes for basic pH, there have been amine-based nanosensors developed which are sensitive in acidic pH [39]. In this case, the reporter molecule 2-thioaniline was sensitive to pH ranging from 3 to 8, although the use of silver nanoparticles led to the same aggregation-induced error as before, limiting the sensor to ± 1 pH unit in living cells. pH-sensitive nanosensors have also been applied to probing the dynamic environment inside cells as the pH changes over time [40], in one case studying the resilience of cancer cells to photodynamic therapy [41]. Endosomes have been specifically targeted for pH sensing [42, 43] by using a nanosensor functionalised with 4-mercaptopyridine for acidic sensing, alongside 2,4-ε-dinitrophenol-L-lysine to target the FcεRI receptor-mediated endocytic pathway.

2.8 Redox-Sensitive Intracellular Nanosensors

In cells, the redox potential is a tightly regulated and compartmentalised intracellular variable. The intracellular redox potential is controlled by a variety of mechanisms, such as couples between oxidised and reduced forms of glutathione, NAD^+/NADH and $NADP^+$/NADPH, or reactive oxygen species (ROS) [44, 45]. Different organelles can have a substantially different redox potential depending on function, for example, more oxidising in the endoplasmic reticulum and more reducing in the mitochondria, to enable the distinct chemistries required in these compartments [46]. When the redox potential of cells is perturbed towards substantially more oxidising potentials, the cells are said to be in a state of oxidative stress, which has been implicated in many diseases and dysfunctions such as inflammation, cancers and neurodegeneration [46, 47]. Redox potential has also been theorised to underpin the entire cascade of programmed cell death (apoptosis), and understanding its regulation or dysregulation could also have implications for cancer treatment [48]. Being able to monitor the intracellular redox potential in single living cells, then, is a desirable outcome.

Microinjected protein crystals of glutathione reductase have been used to monitor the redox potential of the cytoplasm of human fibroblast cells [49], determining it to be approximately −270 mV versus NHE, although the read-out was via relatively insensitive optical microscopy, and the cells were only reported to have survived the injection procedure for a few hours. A modified redox-sensitive green fluorescent protein (roGFP) has also been used to give a read-out of intracellular redox potential [47], but this method has limitations intrinsic to the protein-based nature of the sensor: they require specific per-cell-type genetic engineering, are constrained to a narrow window of potentials [50] and do not survive the relatively oxidising potentials of some subcellular compartments [51]. RoGFP is sensitive to the glutathione redox couple [52], but specific modifications are required in order to detect other species [53]. Additionally, background fluorescence of the cell and medium places a limit on the sensitivity of the technique.

While we previously demonstrated that SERS could be used to investigate the biological significance of redox potential, in the study of a peptide implicated in a human autoimmune disease [33], we have also recently developed a series of SERS nanosensors that can quantitatively report on local redox potential [54].

In this case the reporter is a small redox-active molecule and can exist in either an oxidised or reduced state. The thiol–gold interaction was used to assemble the nanosensors, using hydroquinone and naphthoquinone reporters (Fig. 2.13). Specifically, the naphthoquinone reporter has a distinct series of spectra at a physiologically useful range of redox potentials which exceeds that of fluorescent roGFP. These sensors have been delivered to cells, and we have demonstrated that they can reversibly report on redox potential changes (i.e., both oxidative and reductive changes). We used these sensors to measure changes in intracellular redox

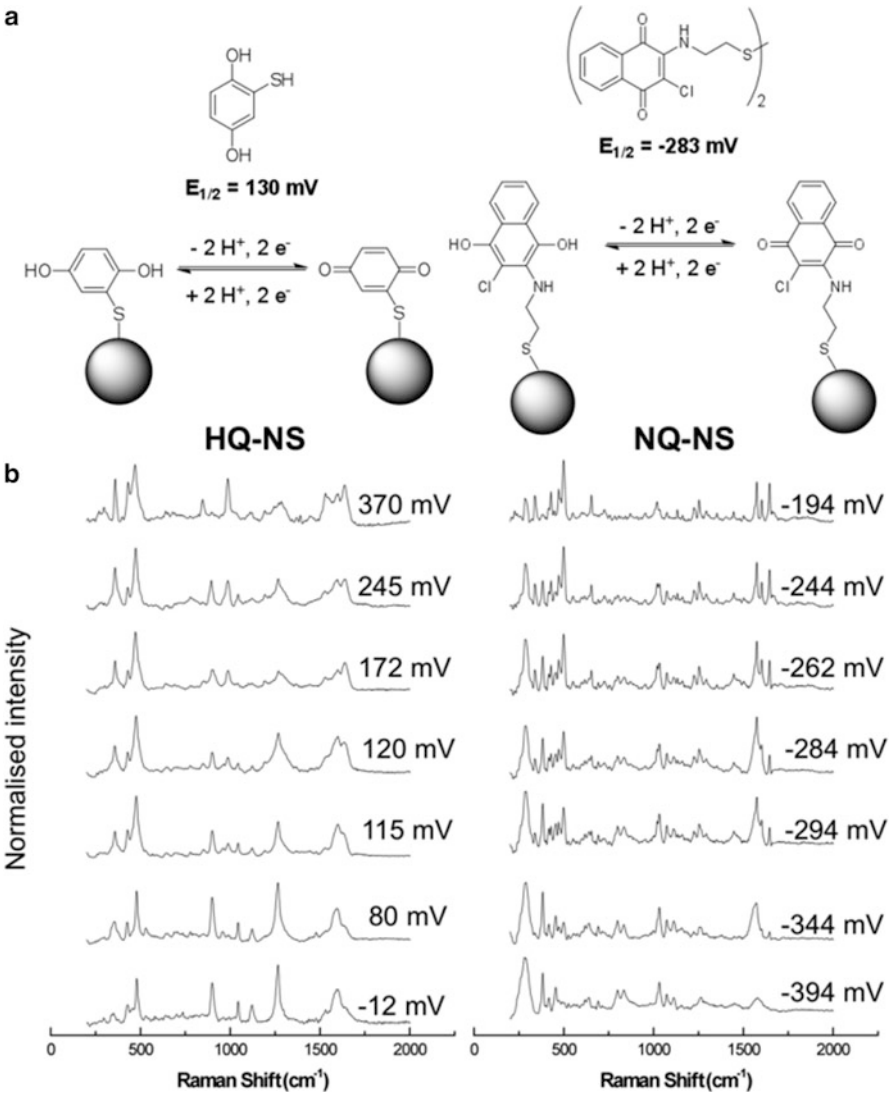

Fig. 2.13 Redox-active SERS nanosensors

potential which result either from exposure to reactive oxygen species or as a result of apoptosis. Figure 2.14 shows the excellent correlation between redox potential measured using SERS nanosensors and the activity of caspase 3/7 (a protease responsible for the execution of apoptosis) in cells undergoing apoptosis.

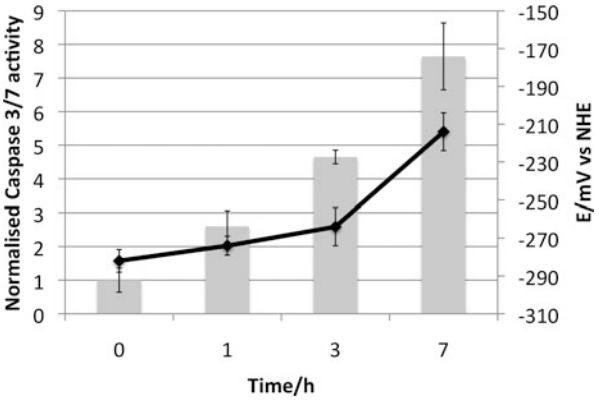

Fig. 2.14 Correlation between redox potential and caspase activity in cells undergoing apoptosis

2.9 Conclusions

Raman spectroscopy of functionalised nanoparticles is an emerging tool in cell biology. There are a variety of nanoparticle architectures and improvements to choose from, with gold nanoshells offering particular promise as single-particle sensing systems with subcellular resolution. The sensors are simple to construct from well-understood gold–thiol ligation chemistry, and reporter molecules and nanoparticles alike are synthetically accessible or commercially available. Nanosensors assembled in this way are taken up readily into cells and show no toxicity or adverse effects over a time span of several days. A wide range of information can be obtained from the use of SERS nanosensors in the study of biological systems, from protein concentration and enzyme activity to intracellular variables such as pH and redox potential. pH sensing is particularly well established, with subcellular resolution data available as accurate as 0.1 pH units. The use of SERS for redox potential monitoring is an emerging technique, which promises to further our understanding of the importance of redox potential in cells and its implication in numerous disease models and cellular processes.

References

1. Watson, W.H., Pohl, J., Montfort, W.R., Stuchlik, O., Reed, M.S., Powis, G., Jones, D.P.: D. P. Redox potential of human thioredoxin 1 and identification of a second dithiol/disulfide motif. J. Biol. Chem. **278**, 33408 (2003)
2. Stolee, J.A., Shrestha, B., Mengistu, G., Vertes, A.: Observation of subcellular metabolite gradients in single cells by laser ablation electrospray ionization mass spectrometry. Angew. Chem. Int. Ed. **51**, 10386 (2012)
3. Lee, Y.E., Kopelman, R.: Optical nanoparticle sensors for quantitative intracellular imaging. Wiley Interdiscip. Rev. Nanomed. Nanobiotechnol. **1**, 98 (2009)
4. Benjaminsen, R.V., Sun, H., Henriksen, J.R., Christensen, N.M., Almdal, K., Andresen, T.L.: Evaluating nanoparticle sensor design for intracellular pH measurements. ACS Nano **5**, 5864 (2011)

5. Rayleigh, L.: On the transmission of light through an atmosphere containing small particles in suspension, and on the origin of the blue of the sky. Philos. Mag. Ser. 5, **47**, 375 (1899)
6. Smith, E., Dent, G., Wiley, J.: Modern Raman Spectroscopy: A Practical Approach. Wiley, Hoboken, NJ (2005)
7. Nobelprize.org, vol. 2013
8. Fleischmann, M., Hendra, P.J., McQuillan, A.J.: Raman spectra of pyridine adsorbed at a silver electrode. Chem. Phys. Lett. **26**, 163 (1974)
9. McQuillan, A.J.: The discovery of surface-enhanced Raman scattering. Notes Rec. R. Soc. **63**, 209 (2009)
10. Jeanmaire, D.L., Van Duyne, R.P.: Surface raman spectroelectrochemistry: part I. Heterocyclic, aromatic, and aliphatic amines adsorbed on the anodized silver electrode. J. Electroanal. Chem. Interf. Electrochem. **84**, 1 (1977)
11. Albrecht, M.G., Creighton, J.A.: Anomalously intense Raman spectra of pyridine at a silver electrode. J. Am. Chem. Soc. **99**, 5215 (1977)
12. Le Ru, E.C., Blackie, E., Meyer, M., Etchegoin, P.G.: Surface enhanced Raman scattering enhancement factors: a comprehensive study. J. Phys. Chem. C **111**, 13794 (2007)
13. Nie, S., Emory, S.R.: Probing single molecules and single nanoparticles by surface-enhanced Raman scattering. Science **275**, 1102 (1997)
14. Qian, X.M., Nie, S.M.: Single-molecule and single-nanoparticle SERS: from fundamental mechanisms to biomedical applications. Chem. Soc. Rev. **37**, 912 (2008)
15. Lombardi, J.R., Birke, R.L.: A unified view of surface-enhanced Raman scattering. Acc. Chem. Res. **42**, 734 (2009)
16. Creighton, J.A., Eadon, D.G.: Ultraviolet-visible absorption spectra of the colloidal metallic elements. J. Chem. Soc. Faraday Trans. **87**, 3881 (1991)
17. Oldenburg, S.J., Averitt, R.D., Westcott, S.L., Halas, N.J.: Nanoengineering of optical resonances. Chem. Phys. Lett. **288**, 243 (1998)
18. Wang, Y., Yan, B., Chen, L.: SERS Tags: Novel Optical Nanoprobes for Bioanalysis. Chem. Rev. **113**, 1391–1428 (2013)
19. Kneipp, K., Wang, Y., Kneipp, H., Perelman, L.T., Itzkan, I., Dasari, R.R., Feld, M.S.: Single molecule detection using surface-enhanced Raman scattering (SERS). Phys. Rev. Lett. **78**, 1667 (1997)
20. Jarvis, R.M., Goodacre, R.: Characterisation and identification of bacteria using SERS. Chem. Soc. Rev. **37**, 931 (2008)
21. Kneipp, K., Haka, A.S., Kneipp, H., Badizadegan, K., Yoshizawa, N., Boone, C., Shafer-Peltier, K.E., Motz, J.T., Dasari, R.R., Feld, M.S.: Surface-enhanced Raman spectroscopy in single living cells using gold nanoparticles. Appl. Spectrosc. **56**, 150 (2002)
22. Ochsenkühn, M.A., Jess, P.R.T., Stoquert, H., Dholakia, K., Campbell, C.J.: Nanoshells for surface-enhanced Raman spectroscopy in eukaryotic cells: cellular response and sensor development. ACS Nano **3**, 3613 (2009)
23. Bain, C., Biebuyck, H., Whitesides, G.: Comparison of self-assembled monolayers on gold: coadsorption of thiols and disulfides. Langmuir **5**, 723 (1989)
24. Bain, C.D., Troughton, E.B., Tao, Y.T., Evall, J., Whitesides, G.M., Nuzzo, R.G.: Formation of monolayer films by the spontaneous assembly of organic thiols from solution onto gold. J. Am. Chem. Soc. **111**, 321 (1989)
25. Rouhana, L.L., Moussallem, M.D., Schlenoff, J.B.: Adsorption of short-chain thiols and disulfides onto gold under defined mass transport conditions: coverage, kinetics, and mechanism. J. Am. Chem. Soc. **133**, 16080 (2011)
26. Coughlin, S.R.: Thrombin signalling and protease-activated receptors. Nature **407**, 258 (2000)
27. Treasure, T., Hill, J.: NICE guidance on reducing the risk of venous thromboembolism in patients admitted to hospital. J. R. Soc. Med. **103**, 210 (2010)
28. Ochsenkuhn, M.A., Campbell, C.J.: Probing biomolecular interactions using surface enhanced Raman spectroscopy: label-free protein detection using a G-quadruplex DNA aptamer. Chem. Commun. **46**, 2799 (2010)

29. Billinghurst, B.E., Oladepo, S.A., Loppnow, G.R.: pH-dependent UV resonance Raman spectra of cytosine and uracil. J. Phys. Chem. B **113**, 7392 (2009)
30. Moger, J., Gribbon, P., Sewing, A., Winlove, C.P.: Feasibility study using surface-enhanced Raman spectroscopy for the quantitative detection of tyrosine and serine phosphorylation. Biochim. Biophys. Acta **1770**, 912 (2007)
31. Benevides, J.M., Tsuboi, M., Bamford, J.K., Thomas, G.J.: Polarized Raman spectroscopy of double-stranded RNA from bacteriophage phi6: local Raman tensors of base and backbone vibrations. Biophys J **72**, 2748 (1997)
32. Yarasi, S., Billinghurst, B.E., Loppnow, G.R.: Vibrational properties of thymine, uracil and their isotopomers. J. Raman Spectrosc. **38**, 1117 (2007)
33. Ochsenkühn, M.A., Borek, J.A., Phelps, R., Campbell, C.J.: Redox potential dependence of peptide structure studied using surface enhanced Raman spectroscopy. Nano Lett. **11**, 2684 (2011)
34. Manoury, B., Mazzeo, D., Fugger, L., Viner, N., Ponsford, M., Streeter, H., Mazza, G., Wraith, D.C., Watts, C.: Destructive processing by asparagine endopeptidase limits presentation of a dominant T cell epitope in MBP. Nat. Immunol. **3**, 169 (2002)
35. Zou, J., Hannier, S., Cairns, L.S., Barker, R.N., Rees, A.J., Turner, A.N., Phelps, R.G.: Healthy individuals have goodpasture autoantigen-reactive T cells. J. Am. Soc. Nephrol. **19**, 396 (2008)
36. Zou, J., Henderson, L., Thomas, V., Swan, P., Turner, A.N., Phelps, R.G.: Presentation of the goodpasture autoantigen requires proteolytic unlocking steps that destroy prominent T cell epitopes. J. Am. Soc. Nephrol. **18**, 771 (2007)
37. Talley, C.E., Jusinski, L., Hollars, C.W., Lane, S.M., Huser, T.: Intracellular pH sensors based on surface-enhanced raman scattering. Anal. Chem. **76**, 7064 (2004)
38. Bishnoi, S.W., Rozell, C.J., Levin, C.S., Gheith, M.K., Johnson, B.R., Johnson, D.H., Halas, N.J.: All-optical nanoscale pH meter. Nano Lett. **6**, 1687 (2006)
39. Wang, Z., Bonoiu, A., Samoc, M., Cui, Y., Prasad, P.N.: Biological pH sensing based on surface enhanced Raman scattering through a 2-aminothiophenol-silver probe. Biosens Bioelectron **23**, 886 (2008)
40. Kneipp, J., Kneipp, H., Wittig, B., Kneipp, K.: Following the dynamics of pH in endosomes of live cells with SERS nanosensors. J. Phys. Chem. C **114**, 7421 (2010)
41. Bálint, Š., Rao, S., Marro, M., Miškovský, P., Petrov, D.: Monitoring of local pH in photodynamic therapy-treated live cancer cells using surface-enhanced Raman scattering probes. J. Raman Spectrosc. **42**, 1215 (2011)
42. Nowak-Lovato, K.L., Rector, K.D.: Targeted surface-enhanced Raman scattering nanosensors for whole-cell pH imagery. Appl. Spectrosc. **63**, 387 (2009)
43. Nowak-Lovato, K.L., Wilson, B., Rector, K.: SERS nanosensors that report pH of endocytic compartments during FcεRI transit. Anal. Bioanal. Chem. **398**, 2019 (2010)
44. Jones, D.P.: Redox sensing: orthogonal control in cell cycle and apoptosis signalling. J. Intern. Med. **268**, 432 (2010)
45. Dooley, C.T., Dore, T.M., Hanson, G.T., Jackson, W.C., Remington, S.J., Tsien, R.Y.: Imaging dynamic redox changes in mammalian cells with green fluorescent protein indicators. J. Biol. Chem. **279**, 22284 (2004)
46. Menon, S.G., Goswami, P.C.: A redox cycle within the cell cycle: ring in the old with the new. Oncogene **26**, 1101 (2006)
47. Gutscher, M., Pauleau, A.-L., Marty, L., Brach, T., Wabnitz, G.H., Samstag, Y., Meyer, A.J., Dick, T.P.: Real-time imaging of the intracellular glutathione redox potential. Nat. Methods **5**, 553 (2008)
48. Mallikarjun, V., Clarke, D.J., Campbell, C.J.: Cellular redox potential and the biomolecular electrochemical series: a systems hypothesis. Free Radic. Biol. Med. **53**, 280 (2012)
49. Keese, M.A., Saffrich, R., Dandekar, T., Becker, K., Schirmer, R.H.: Microinjected glutathione reductase crystals as indicators of the redox status in living cells. FEBS Lett. **447**, 135 (1999)
50. Lohman, J.R., Remington, S.J.: Development of a family of redox-sensitive green fluorescent protein indicators for use in relatively oxidizing subcellular environments. Biochem. **47**, 8678 (2008)

51. Hwang, C., Sinskey, A.J., Lodish, H.F.: Oxidized redox state of glutathione in the endoplasmic reticulum. Science (New York, NY) **257**, 1496 (1992)
52. Meyer, A.J., Brach, T., Marty, L., Kreye, S., Rouhier, N., Jacquot, J.-P., Hell, R.: Redox-sensitive GFP in Arabidopsis thaliana is a quantitative biosensor for the redox potential of the cellular glutathione redox buffer. Plant J. **52**, 973 (2007)
53. Morgan, B., Sobotta, M.C., Dick, T.P.: Measuring EGSH and H_2O_2 with roGFP2-based redox probes. Free Radic. Biol. Med. **51**, 1943 (2011)
54. Auchinvole, C.A.R., Richardson, P., McGuinnes, C., Mallikarjun, V., Donaldson, K., McNab, H., Campbell, C.J.: Monitoring intracellular redox potential changes using SERS nanosensors. ACS Nano **6**, 888 (2011)

http://www.springer.com/978-3-319-02771-5

Nanoscale Sensors

Li, S.; Wu, J.; Wang, Z.M.; Jiang, Y. (Eds.)

2013, XII, 281 p. 165 illus., 95 illus. in color., Hardcover
ISBN: 978-3-319-02771-5